



Spectrum of Chest CT Findings in Covid-19 Patients: Relationship to the Patient's Age Group and Duration of Infection in Al-Dhafra Hospitals, Abu Dhabi

Nehar Ranjan Chakraborty^a, Ahmed Saeed Al Hurmuzi^a, Ashraf Alakkad^{b*} and Feras Youssef Al Zoabi^b

^a *Department of Diagnostic Radiology, Madinat Zayed Hospital, AL Dhafra Region, UAE.*

^b *Department of Internal Medicine, Madinat Zayed Hospital, AL Dhafra Region, UAE.*

Authors' contributions

This work was carried out in collaboration among all authors. All authors read and approved the final manuscript.

Article Information

DOI: 10.9734/JAMMR/2022/v34i234836

Open Peer Review History:

This journal follows the Advanced Open Peer Review policy. Identity of the Reviewers, Editor(s) and additional Reviewers, peer review comments, different versions of the manuscript, comments of the editors, etc are available here: <https://www.sdiarticle5.com/review-history/92709>

Original Research Article

Received 12 August 2022
Accepted 20 October 2022
Published 21 October 2022

ABSTRACT

Purpose: This study aims to identify chest CT findings among asymptomatic and symptomatic COVID-19-positive patients in Al Dhafra Hospitals and review the common CT findings in relation to the different age groups of the patients and the duration of their symptoms.

Methods: Data from 301 consecutive patients whose COVID-19 infection was confirmed using an RT-PCR test, and who subsequently underwent a chest CT and presented to our hospital, were collected from April, 1 to May 31, 2020. They were further classified according to the time after the onset of the initial symptoms, namely stage-1 (0–4 days); stage-2 (5–8 days); stage-3 (9–14 days), and stage-4 (14+ days), and according to the age of the patient in four groups (Group A- <18 years, Group B- 18–44 years, Group C- 45–59 years, and Group D- ≥60 years). We analyzed the prevalence, distribution, type of abnormal lung findings, and extent of the involvement of affected lobes through Ground-Glass Opacities (GGO), crazy-paving pattern, and consolidation in five categories of percentual severity by semi-quantitative CT score (maximum CT score, 25).

Results: Multiple small patchy, rounded, pure Ground-Glass Opacities (GGO) and mixed GGO with consolidations were the main HRCT signs in 231 patients with confirmed COVID-19 infections. Both

of these were predominant patterns in the young, middle, and elderly groups (<18 to >60 years). However, crazy paving patterns were more common in groups ages 45 to <60. The peripheral disease distribution was seen in 100% of cases, and both peripheral and central types of distribution of opacities were most common in the elderly group (>60 years old), at 73.3%. Bilateral involvements were common in all groups, but unilateral involvement was fairly common in groups ages <18 to 44 years old. Both the mean number of lesions and CT score were higher in 44 to <69 years and >69 years aged groups than in <18 to 44 years old, and lower lobes showed relatively higher numbers of lesions and CT score than other lobes in all age groups.

Normal CT findings among symptomatic patients were seen in the early stage (0–4 days) and progressive stage (5-8 days) of the disease, at 36.3% and 6.6%, respectively. Peripheral mixed GGO with consolidation and pure GGO were the most important imaging manifestations in the early and progressive stages of the disease. CT features of the lesions were variable in the peak (9-13 days) and late stages (14+ days), showing a mixture of GGO, crazy-paving pattern, consolidation, and linear opacities. Both the “Reverse Halo sign” and “Halo sign” were seen, predominately in the early stage of the disease (0 to 8 days) in 52 patients (22.5%) and 16 patients (6.9%), respectively. The number of lesions per capita, meaning the number of lesions in different lobes of both lungs and the CT score, were higher in the progressive and peak stages of the disease than in the early stage, and then gradually decreased in the late stage of the disease. We also observed a relatively greater number of lesions in both lower lobes compared to the upper lobes and a smaller number of lesions in the right middle lobe at all stages.

Conclusion: The most common HRCT findings in patients with COVID-19 pneumonia were peripheral, bilateral, rounded pure ground glass opacities, and mixed GGO with consolidation. The early stages of the disease may present with normal CT chest findings. Chest HRCT manifestations in patients with COVID-19 are related to the patient’s age and the duration of the symptoms, and HRCT signs are relatively milder in younger patients and in the early stage of the disease. CT could be a useful tool for evaluating the changes in pulmonary abnormalities in patients at different stages and in different age groups (especially elderly groups) for optimal management.

Keywords: COVID-19; ground-glass opacities (GGO); halo sign; consolidation.

1. INTRODUCTION

“In December 2019, a lower respiratory tract febrile illness of unknown origin was reported in a cluster of patients in Wuhan City, Hubei Province, China. A novel strain of Coronavirus isolated from the broncho-alveolar lavage of the patients was determined to be responsible for the outbreak. Pulmonary syndrome was later named Coronavirus disease 2019 (COVID-19) by the World Health Organization” [1,2]. “On January 29, the Ministry of Health and Prevention (MoHAP) confirmed the UAE’s first case of COVID-19 disease [3]. In early March 2020, the WHO declared this outbreak a global pandemic. According to the World Health Organization (WHO), on April 27, 2021, there had been 147,539,302 confirmed cases of COVID-19, including 3,116,444 deaths” [4].

SARS-CoV-2 is an enveloped single-stranded RNA virus [5,6]. The clinical presentation ranges from asymptomatic, mildly symptomatic cases to severely ill [7,8]. “Imaging findings of COVID-19 closely resemble other viral pneumonia. Clinical recovery is associated with the gradual

resorption of pulmonary opacities. In some patients, the clinical course is complicated by acute respiratory distress syndrome (ARDS) or pulmonary embolism, the main causes of death” [9,10]. “Chest high-resolution computed tomography (HRCT) is an important method for detecting lung abnormalities. It plays an irreplaceable role in the screening of suspected patients, the diagnosis and differential diagnosis of diseases, clinical classification, assessment of disease progression, detection of pulmonary complications, and follow-up after discharge” [11].

The present study aims to identify chest CT findings among asymptomatic and symptomatic patients and review the common CT findings in relation to the patients’ different age groups and the duration of their symptoms.

2. METHODOLOGY

2.1 Data Collection

This retrospective study was approved by the Ethics Review Committee of the Department of

Health, Abu Dhabi, UAE. The informed consent was waived off as per the committee. We collected clinical and laboratory data for analysis, derived from an electronic medical record system, concerning patients who presented to our hospital between 1st April 22, 2020, and May 31, 2020, and who had been confirmed as being COVID-19 infected using an RT-PCR test. Chest HRCT images were evaluated using the Picture Archiving and Communication Systems (PACS). The study population solely includes patients with COVID-19 positive results who have undergone chest CT, irrespective of their age.

2.2 CT Protocol

CT scans were performed at the end-inspiration level with patients in a supine position and with their arms raised. Scanning parameters were tube voltage (100 kV), tube current (100–240 mA), slice thickness (5 mm), interval between slices (5 mm), consecutive 1.25 mm slices for high-resolution reconstruction scan, and scanning time (<5 s).

2.3 HRCT Image Analysis

“Two radiologists, with more than 10 years of experience in radiology, independently reviewed CT images in PACS. The readers categorized the predominant patterns on CT scans (lung lesions were categorized using the Fleischner society glossary of terms for thoracic imaging) as ground-glass opacification (GGO, hazy areas of increased attenuation without obscuration of the underlying vessels), crazy-paving pattern (GGO with interlobular and intralobular septal thickening), consolidation (homogeneous opacification of the parenchyma with obscuration of the underlying vessels), and linear opacities (disordered arrangement of coarse linear or curvilinear opacities or fine subpleural reticulation). Other abnormalities, including opacities with a rounded morphology or opacities with a “Halo” or “reverse halo” sign, were also identified” [12]. On the scans, some other minor signs, such as air bronchogram, cavitation, bronchiectasis, pleural effusion, pericardial effusion, pneumothorax, and mediastinal lymphadenopathy (defined as a lymph node greater than 1 cm in short-axis diameter) were also noted.

In this study, lung lobe distribution information included the right upper lobe, the right middle lobe, the right lower lobe, the left upper lobe, and the left lower lobe. The distribution of the lung

field included the periphery (the outer one-thirds region of the lung), the central zone (the area inside the inner two-third region of the lung), and whether the peripheral and central zones were affected simultaneously.

“The severity of the disease, according to the extent of GGO, crazy-paving pattern, and consolidation at thin-section CT, was also evaluated. Bilateral lungs were divided into five lung zones according to the anatomical structure of the lung: left upper lobe, left lower lobe, right upper lobe, right middle lobe, and right lower lobe. Each lung lobe was assigned a score based on the following criteria: score 0, 0% involvement; score 1, less than 5% involvement; score 2, 5% to less than 25% involvement; score 3, 25% to less than 50% involvement; score 4, 50% to less than 75% involvement; and score 5, 75% or greater involvement. The summation of the scores provided a semi-quantitative evaluation for overall lung involvement (maximal CT score for both lungs was 25)” [13,14].

After evaluation, the scans were categorized according to the period between the onset of initial symptoms and the CT scans: stage-1 (0–4 days, n=171); stage-2 (5–8 days, n=91); stage-3 (9–13 days, n=20); stage-4 (14+days, n=6). Chest HRCT findings of infected patients were also categorized in four age groups (Group A<18 years--n= 1), B (18–44 years--n= 162), C (45–59 years--n= 115), D (≥60 years--n= 23) and compared.

2.4 Statistical Analysis

Measurement data are expressed as mean ± standard deviation, and numerical data are described as frequency. We mainly used one-way ANOVA analysis of variance (post-hoc multiple comparisons using least significant difference [LSD] and a q-test), Kruskal-Wallis test among multiple groups to compare the HRCT signs of COVID-19-infected patients within different age groups and at different stages, and noticed the difference was statistically significant with a P-value <0.05.

3. RESULTS

3.1 Baseline Information

Our population included 301 consecutive patients who were COVID-19 positive (using an RT-PCR as a gold standard test) and who underwent chest CT, irrespective of their age. Out of them

were 243 men (80.7%) and 58 women (19.26%), ranging from 15 to 91 years old (Mean age, 44.5 ± 11.6 years). Among them, according to the period between the onset of initial symptoms and the CT scans: stage-1 (0–4 days, n=170); stage-2 (5–8 days, n=91); stage-3 (9–13 days, n=20); stage-4 (14+days, n=6). Thirteen patients (4.32%) were asymptomatic at the time of the CT scan.

Chest HRCT findings of infected patients were categorized in four age groups (Group A<18 years--n= 1), B (18–44 years--n= 162), C (45–59 years--n= 115), and D (≥ 60 years--n= 23) and compared. The most prevalent presenting symptoms at onset of illness were dry cough (75.7%), fever (71.1%), fatigue (54.5%), sore throat (53.8%), dyspnea (21.9%), abdominal pain/diarrhea (3.4%), and anosmia (2.0%). Less common symptoms included expectoration, hemoptysis, abdominal pain and diarrhea, headache, nausea and vomiting, and palpitation (Table 1).

Laboratory results showed that 56 (18.6%) patients had abnormal white blood cell (normal value $1.5-4 \times 10^9/L$) counts (decreased WBC counts, n=51; elevated WBC counts, n=5). We also noticed low platelet count (normal value $1.5-4 \times 10^9/L$) in 30 patients (9.9%), elevated CRP (normal value ≤ 5 mg/L) in 188 patients (62.5%), and high d-dimer (normal value ≤ 0.5 mcg/mL) in 79 patients (26.2%) (Table 1).

3.2 HRCT Evaluation

A total of 301 patients who had undergone HRCT scan were included in the assessment. The scans were positive in 231 patients (76.7%) and negative in 70 patients (23.3%).

Mixed ground glass opacities (GGO) with consolidation pattern, n= 163/231 (70.6%) were the most common HRCT manifestation among the positive patients involved in our study. Pure ground glass pattern was seen in (44.2%), followed by crazy paving pattern, in 24.2%. Both “Reverse Halo signs” and “Halo signs” were seen, predominately in the early stage of the disease (0 to 8 days) in 52 patients (22.5%) and in 16 patients (6.9%), respectively.

The patterns of the opacities were rounded at 79.7% and linear in 21.6% of cases. The peripheral disease distribution was seen in 100% of cases (n=231), and both in central and peripheral were 37.2%.

In asymptomatic patients (n=13), four cases showed negative CT findings. The remaining nine cases show predominately rounded, pure GGO (4/9) and mixed GGO with consolidation (4/9) in peripheral distribution (9/9). Both Halo (2/9) and reverse halo signs (1/9) were also seen.

Table 1. Demographic data, Initial symptoms, and Laboratory Investigations of patient

Gender	
Male	243 (80.7%)
Female	58 (19.26%)
Age	
Age	Range = 15 - 91 years
Mean \pm Standard Deviation	44.5 ± 11.6
Initial symptoms	
Dry cough	n= 228 (75.7%)
Fever	n= 214 (71.1%)
Fatigue	n= 164 (54.5%)
Sore throat	n= 162(53.8%)
Dyspnea	n= 67(21.9%)
Abdominal pain/Diarrhea	n= 11(3.4%)
Anosmia	n= 6 (2.0%)
Laboratory Investigations	
Abnormal WBC count n= 56 (18.6%)	
High WBC count	n=5(11.7%)
Low WBC count	n=51 (16.9%)
Low Platelet	n=30 (9.9%)
Elevated C-Reactive Protein (CRP)	n=188 (62.5%)
High D-Dimer	n=79 (26.2%)

Table 2. Overall CT findings (Opacities) & distribution of lesions (n= 301)

Normal CT findings	n= 70 (23.3%)
Abnormal CT findings	n= 231 (76.7%)
Types of Lesions	
Pure GGO	n= 102 (44.2%)
Mixed GGO with consolidation	n= 163 (70.6%)
Only consolidation	n= 1 (0.4%)
GGO with crazy paving	n= 56 (24.2%)
Reverse Halo sign	n= 52 (22.5%)
Halo sign	n= 16 (6.9%)
Pattern of Lesion	
Rounded	n= 184 (79.7%)
Linear	n= 50 (21.6%)
Distribution of Lesions	
Peripheral	n= 231 (100%)
Only central	n= 0(0%)
Peripheral + central	n= 86 (37.2%)
Bronchiectasis	n= 26(11.3%)
Cavitation	n= 1(0.4%)
Pleural effusion	n= 3(1.3%)
Pericardial effusion	n= 0 (0%)
Pneumothorax	n= (0%)
Lung Involvement	
Unilateral	n= 20 (8.7%)
Bilateral	n= 211 (91.3%)

The chest HRCT findings of infected patients were then categorized into four age groups (Group A<18 years--n= 1), B (18–44 years--n= 162), C (45–59 years--n= 115), D (≥60 years--n= 23) and compared in terms of bilateral/unilateral lung and lobe involvement, distribution, pattern & number of opacities, and CT score

Table 3. Overall CT findings (Opacities) & distribution of lesions in different age groups (n= 301)

	Group A (<18 years) n=1	Group B (18-44 years) n= 162	Group C (45- 59 years) n=115	Group D (>60 years) n=23
CT findings				
Normal	1	47 (29.0%)	18 (15.7%)	4 (17.4%)
Abnormal	0	115 (71%)	97 (84.3%)	19 (82.6%)
Types of opacities				
Pure GGO	0	47(40.9%)	41(42.3%)	12(63.2%)
Mixed GGO with consolidation	0	81 (70.4%)	70 (72.2%)	12 (63.2%)
Only consolidation	0	1 (0.9%)	0 (0%)	0 (0%)
GGO with crazy paving	0	16 (13.9%)	34 (35.1%)	6 (31.6%)
Reverse Halo sign	0	27(23.5%)	23(23.7%)	2(10.5%)
Halo sign	0	11(9.5%)	3(3.1%)	2(10.5%)
Pattern of lesions				
Rounded	0	98 (85.2%)	70 (72.2%)	16 (63.2%)
Linear	0	17 (14.8%)	30 (30.9%)	3 (15.8%)
Distribution of lesions				
Peripheral	0	115 (100%)	97 (100%)	19(100.0%)
Only Central	0	0 (0%)	0 (0%)	0 (0%)
Peripheral + central	0	39 (33.9%)	33 (34.0%)	14 (73.6%)
Others				
Bronchiectasis	0	9 (7.8%)	16 (16.5%)	1(5.3%)
Pleural effusion	0	0 (0%)	2 (2.1%)	1 (5.3%)
Pericardial effusion	0	0 (0%)	0 (0%)	0 (0%)
Pneumothorax	0	0 (0%)	0 (0%)	0 (0%)
Lymphadenopathy (mild)	0	7 (6.1%)	5 (5.2%)	3 (15.8%)

The lung shows bilateral involvement in 91.3% of cases (n=211), consolidation alone in 0.5%, bronchiectasis in 11.3%, pleural effusion in 1.3% (n=3, unilateral in 2 and bilateral in one case, seen only in stage-4 of the disease), and cavitation in 0.4% (Table 2).

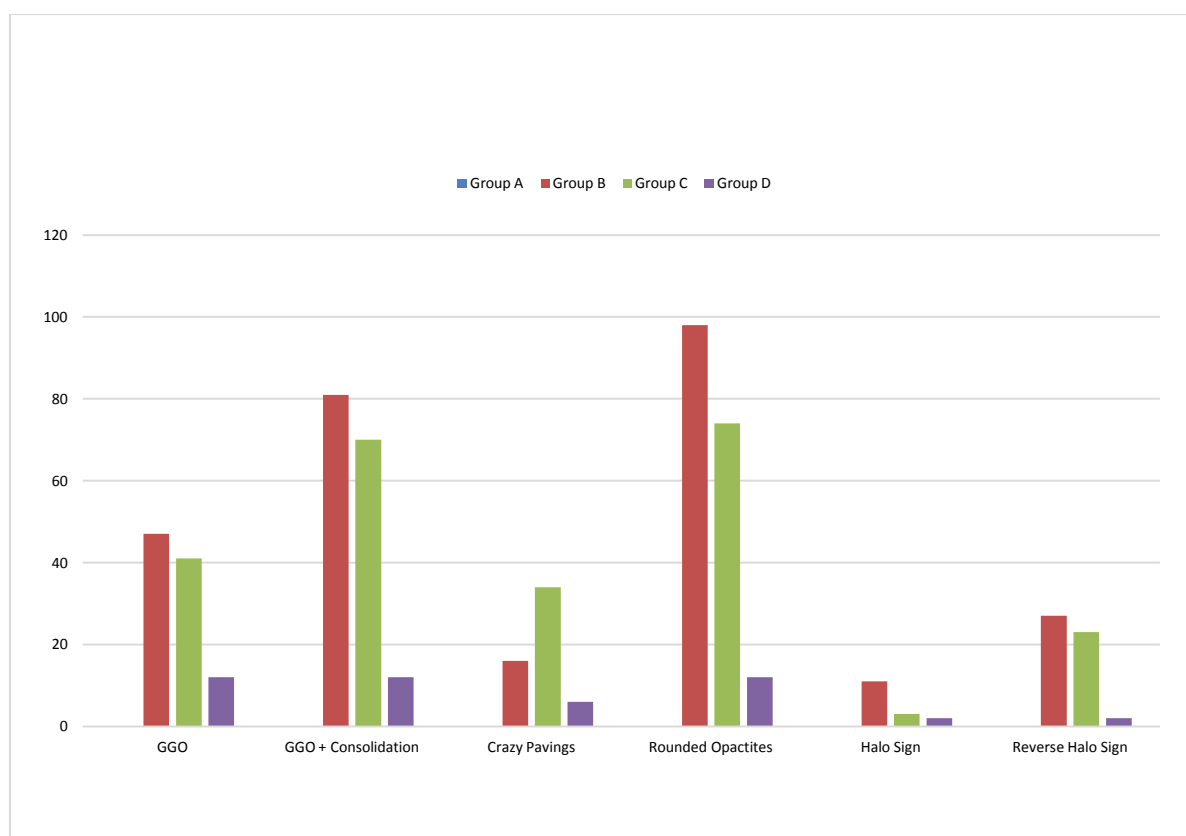
In Group A, we found only one symptomatic 15-year-old patient, who showed negative CT findings. Group B (18-44 years) presented the highest number of negative CT findings (47/162-29%), followed by Groups C (18/115) and D (4/23). We identified 211 patients (91.3%) with bilateral lung involvement and 20 (8.7%) with unilateral lung involvement. There were fewer cases of unilateral lung involvement in Groups C and D than in Group B. Although, bilateral lung involvement was common in all groups (except for Group A). Group C showed the highest number, with almost all patients showing signs of involvement (96/97), followed by Groups D (89.5%) and B (85.2%) (Table 4).

Among the density characteristics of each lesion, as detailed in Table 3, mixed GGO with consolidation is the most commonly observed

HRCT finding in patients of all age groups (C, B, and D, respectively). Pure GGO were more common in Group D (62.3%), and GGO with crazy paving were common in Groups C and D (35% and 31.6%, respectively). The rounded pattern was the most prevalent pattern in all age groups and was highest in Group B (85.2%). A linear pattern was most commonly seen in Group C.

In our study, we found a peripheral distribution of lesions in all patients in all age groups. However, centrally located lesions, along with peripheral ones, were most commonly seen in the elderly Group D, in 73.6% of cases, and least commonly in the younger Group B (33.9%).

Reverse Halo signs (RHS) and Halo signs (HS) were found in all age groups (B, C, and D). RHS were almost found in the same incidence in Groups B (23.5%) and C (23.7%), while fewer were found in Group D (10.5%). On the other hand, Halo signs were found almost equally distributed in Groups D and B (10.5% & 9.5%, respectively) and were fewer in Group C (Table 3)



Graph I. Patterns of Abnormality in CT (Age)

Bronchiectasis was observed in the highest percentage in Group C (16.5%). We also found small pleural effusion in Groups C (2.1%) and D (5.3%), and no pleural effusion in the young age Group B.

The number of lesions per capita and the mean number of lesions in different lobes of both lungs were higher in Groups C and D than in Group B. However, there was no significant difference in the number of lesions in the different age groups ($P > 0.05$). We also observed a relatively greater number of lesions in both lower lobes than in the upper lobes and a smaller number of lesions in the right middle lobe in all age groups, which were also not statistically significant (Table 4).

The same observation as in the distribution and number of lesions was reflected in the CT score in the different age groups. It showed no significant difference in the mean number between both lungs and the different lobes in different groups (Table 5).

We then analyzed the data according to the period between the onset of initial symptoms and the CT scans: Stage 1 (0–4 days, $n=170$), Stage 2 (5–8 days, $n=91$), Stage 3 (9–13 days, $n=20$), and Stage 4 (14+days, $n=6$). In most patients, the lesions were present bilaterally in multiple lobes, with the lowest rate (92.9%) at Stage 2 and the highest (100%) at Stage 4. In the early stage of the disease (Stage 1), CT scans showed 15.6% of unilateral lung involvement.

Table 4. Distribution of number of lesions in the lungs in different age groups

	Group A (<18 years) n =1	Group B (18-44 years) n= 162	Group C (45- 59 years) n=115	Group D (>60 years) n=23	P
RUL	0	2.76 ± 0.92	4.91 ± 2.95	4.47 ± 2.99	0.575
RML	0	1.64 ± 2.01	2.36 ± 2.06	2.41 ± 2.38	0.126
RLL	0	4.05 ± 3.06	5.87 ± 2.79	5.24 ± 2.53	0.906
LUL	0	2.66 ± 3.19	3.81 ± 2.76	4.12 ± 2.76	0.787
LLL	0	4.03 ± 3.03	5.19 ± 2.81	4.81 ± 2.70	0.943
Total	0	1773	2000	353	0
No. of lesions per Capita	0	3.03±0.92	4.44±1.23	4.21±0.97	0
Unilateral	0	18 (15.6%)	1 (1.0%)	1(1.0%)	0
Bilateral	0	98 (85.2%)	96 (98.9%)	17 (89.5%)	0

The mean difference is significant at a level of 0.05.

Data were analyzed using one-way ANOVA analysis of variance

Table 5. CT severity score in different age groups

	Group A (<18 years) n =1	Group B (18-44 years) n= 162	Group C (45- 59 years) n=115	Group D (>60 years) n=23	P
Right lung	0	1.29 ± 1.26	1.88 ± 1.61	1.79 ± 1.21	0.704
Left lung	0	1.48 ± 1.28	2.11 ± 1.15	2.26 ± 1.29	0.792
Right upper lobe	0	1.19±1.21	1.91 ± 1.07	1.58 ± 1.04	0.788
Right middle lobe	0	0.86 ± 1.02	1.17 ± 0.96	1.21 ± 0.95	0.6416
Right lower lobe	0	1.83 ± 1.34	2.56 ± 1.01	2.58 ± 1.18	0.9437
Left upper lobe	0	1.15 ± 1.19	1.82 ± 1.15	2.05 ± 1.36	0.4831
Left lower lobe	0	1.81 ± 1.28	2.41 ± 1.07	2.47 ± 1.36	0.8875

The mean difference is significant at a level of 0.05

Data were analyzed using one-way ANOVA analysis of variance

The most frequent CT findings of COVID-19 pneumonia were GGO, mixed GGO with consolidation, and crazy-paving pattern. The predominant patterns of abnormality changed over time. In the early stage (Stage 1), pure GGO and mixed GGO with consolidation were the most important imaging manifestations (55% and 63.3%, respectively), and in some patients, we noted a crazy-paving pattern (22.9%), as well as Reverse halo signs (21.1%) and Halo signs (6.4%). Pure GGO were found in the highest percentage at all stages.

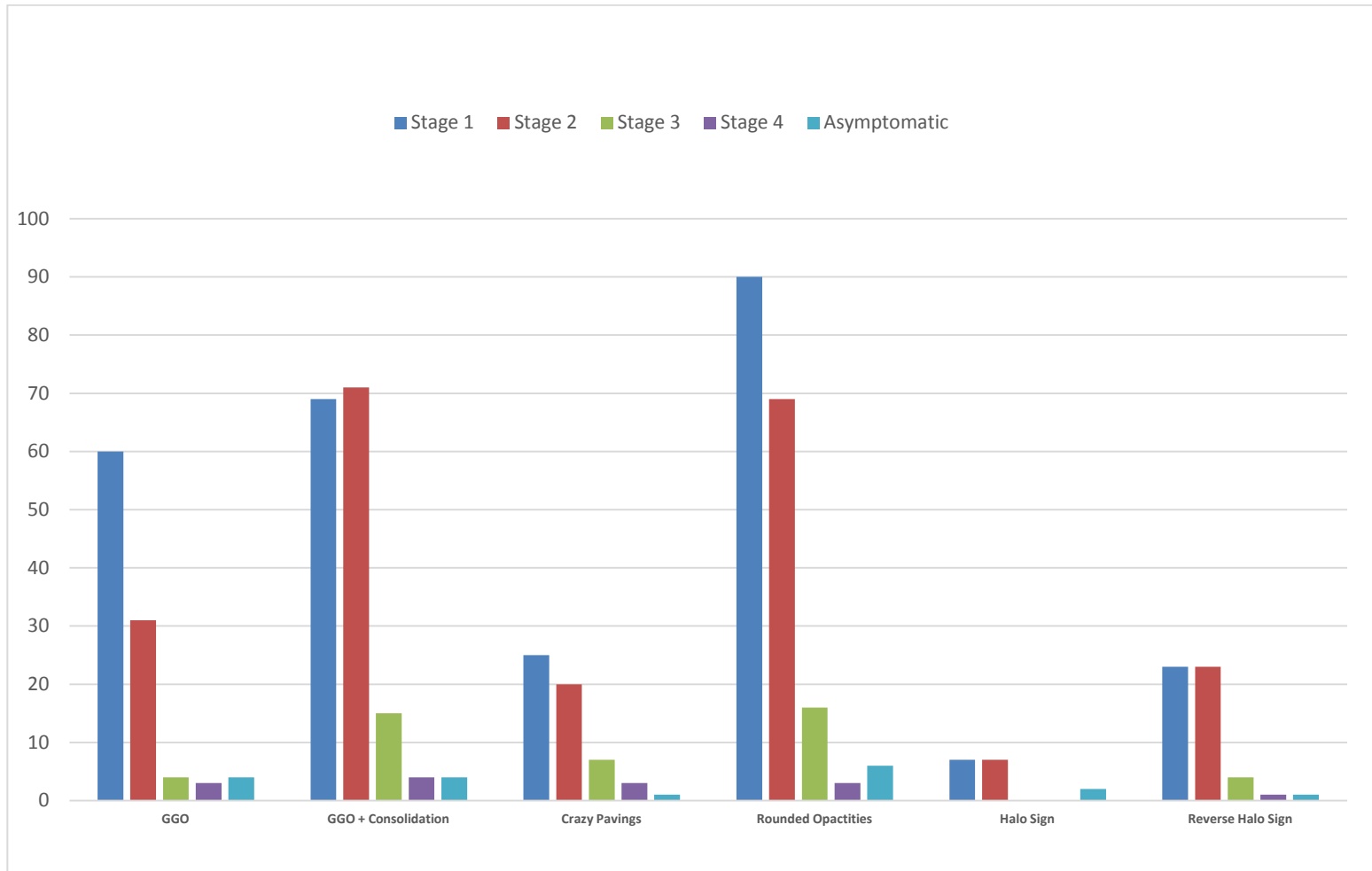
At Stages 2 and 3, mixed GGO with consolidation were the predominant pattern (83.5% and 83.3%, respectively) and tended to decrease in later stages, reaching 44.4% at Stage 4. GGO with crazy paving showed a mild increase in distribution between Stage 1 (22.9%) and Stage 4 (50%). Reverse Halo signs were

seen at Stage 1(21.1%), Stage 2 (22.2%), and Stage 3 (16.7%) of the disease. On the other hand, Halo signs were only found in Stage 1 (6.4%) and Stage 2 (8.2%) of the disease. Bronchiectasis was a common finding in Stage 4 patients (100%). We also found three patients with small pleural effusion (one bilateral and two unilateral), all of which were Stage 4 patients (50%.) (Table 6).

We observed that the mean number & distribution of lesions and the CT score were progressively higher from Stage 1 to Stage 3, where it reached the maximum before decreasing. These observations were seen between the stages, lobes of each lung, and both lungs. The number of lesions and the CT score were relatively higher in the lower lobes of both lungs. We didn't find any statistically significant difference between them. (Tables 7 & 8).

Table 6. Overall CT findings (Opacities) & distribution of lesions at different stages of the disease (n= 301)

	Stage-1 (0-4 days) n= 171	Stage-2 (5-8 days) n=91	Stage-3 (9-13 days) n=20	Stage-4 (14+ days) n=06	Asymptomatic n=13
Age (years)	43.5±12.0	45.5±10.1	45.0±8.6	55.1±10.4	48.8 ± 21.7
CT findings					
Normal	62 (36.3%)	06 (6.6%)	02 (10.0%)	0 (0%)	4 (30.8%)
Abnormal	109 (63.7%)	85 (93.4%)	18 (90%)	06 (100%)	9 (69.2%)
Types of Opacities					
Pure GGO	60 (55.0)	31 (36.5%)	4 (22.2%)	3(50%)	4 (44.4%)
Mixed GGO with consolidation	69 (63.3%)	71 (83.5%)	15 (83.3%)	4 (66.7%)	4 (44.4%)
Only consolidation	1 (0.9%)	0 (0%)	0 (0%)	0 (0%)	0 (0%)
GGO with crazy paving	25 (22.9%)	20 (23.5%)	7 (38.9%)	3 (50%)	1 (11.1%)
Reverse Halo sign	23 (21.1%)	23 (27.1%)	4 (22.2%)	1 (16.7%)	1 (11.1%)
Halo sign	7 (6.4%)	7 (8.2%)	0 (0%)	0 (0%)	2 (22.2%)
Pattern of lesions					
Rounded	90 (82.6%)	69 (81.2%)	16 (88.9%)	3 (50%)	6 (100%)
Linear	21(19.3%)	14 (16.5%)	9 (50%)	5 (83.3%)	1 (11.1%)
Distribution of lesions					
Peripheral	109(100%)	85 (100%)	20 (100%)	6 (100.0%)	9 (100%)
Only Central	0 (0%)	0 (0%)	0 (0%)	0 (0%)	0 (0%)
Peripheral + central	40 (36.7%)	33 (38.8%)	8(44.4%)	1 (16.7%)	4 (44.4%)
Others					
Bronchiectasis	13 (11.9%)	7 (8.2%)	5 (27.8%)	6 (100%)	0 (0%)
Pleural effusion	0	0 (0%)	0 (0%)	3 (50.0%)	0 (0%)
Pericardial effusion	0	0 (0%)	0 (0%)	0 (0%)	0 (0%)
Pneumothorax	0	0 (0%)	0 (0%)	0 (0%)	0 (0%)



Graph II. Patterns of Abnormality in CT (Duration of Symptoms)

Table 7. Distribution of number of lesions in the lungs at different stages (duration of symptoms)

	Stage-1 (0-4 days) n= 171	Stage-2 (5-8 days) n=91	Stage-3 (9-13 days) n=20	Stage-4 (14+ days) n=06	Asymptomatic n=13
Right Lung	3.07 ± 3.06 (1150)	4.14 ± 2.83 (1036)	5.56 ± 3.06 (218)	3.46 ± 2.97 (45)	2.26 ± 2.85 (52)
Left Lung	3.28 ± 2.96 (826)	4.48 ± 2.81 (734)	6.65 ± 3.35 (173)	3.57 ± 2.26 (25)	2.07 ± 2.02 (31)
RUL	3.10 ± 3.06 (388)	4.55 ± 2.89 (378)	6.08 ± 3.34 (79)	5.50 ± 3.20 (22)	2.50 ± 3.08 (20)
RML	1.65 ± 1.95 (204)	2.50 ± 2.31 (210)	3.23 ± 2.04 (40)	1.60 ± 1.50 (8)	0.88 ± 1.05 (7)
RLL	4.43 ± 3.31 (558)	5.40 ± 2.45 (448)	7.46 ± 1.45 (97)	3.75 ± 1.92 (15)	3.57 ± 3.25 (25)
LUL	2.46 ± 2.66 (312)	4.11 ± 2.86 (337)	5.85 ± 4.28 (76)	3.33 ± 2.62 (10)	1.13 ± 1.69 (9)
LLL	4.11 ± 3.03 (514)	4.84 ± 2.72 (397)	7.46 ± 1.69 (97)	3.75 ± 1.92 (15)	3.14 ± 1.81 (22)
Unilateral	17 (15.6%)	2 (7.1%)	0	0	1
Bilateral	102 (93.6%)	79 (92.9%)	17 (94.5)	6 (100%)	7 (53.8%)

*The mean difference is significant at a level of 0.05.
Data were analyzed using one-way ANOVA analysis of variance*

Table 8. CT severity score at different stages (duration of symptoms)

	Stage-1 (0-4 days) n= 171	Stage-2 (5-8 days) n=91	Stage-3 (9-13 days) n=20	Stage-4 (14+ days) n=06	Asymptomatic n=13	P Value
Right lung	1.34 ± 1.21	1.81 ± 1.22	2.31 ± 1.23	2.06 ± 1.27	1.19 ± 1.19	0.797
Left lung	1.53 ± 1.24	2.01 ± 1.21	2.80 ± 1.17	2.50 ± 0.96	1.22 ± 1.08	0.98
Right upper lobe	1.21 ± 1.12	1.84 ± 1.16	2.27 ± 1.06	2.17 ± 1.07	1.00 ± 0.94	0.851
Right middle lobe	0.89 ± 0.97	1.17 ± 1.05	1.33 ± 0.79	1.17 ± 1.07	0.56 ± 0.50	0.774
Right lower lobe	1.92 ± 1.27	2.41 ± 1.11	3.33 ± 0.87	2.83 ± 1.07	2.00 ± 1.41	0.973
Left upper lobe	1.24 ± 1.22	1.73 ± 1.16	2.20 ± 1.17	2.33 ± 1.11	0.78 ± 0.92	0.83
Left lower lobe	1.82 ± 1.19	2.29 ± 1.20	3.40 ± 0.80	2.67 ± 0.75	1.67 ± 1.05	0.966

*The mean difference is significant at a level of 0.05.
Data were analyzed using one-way ANOVA analysis of variance*

4. DISCUSSION

A wide spectrum of clinical manifestations can be seen with COVID-19 [15]. The nasal epithelium is one of the first sites of infection with SARS-CoV-2 [16,17]. In our study, respiratory symptoms like dry cough (75.7%) and fever (71.1%) were the most common manifestations of COVID-19. In Grant et al.'s systematic review, performed on 24,410 adults with confirmed COVID-19 infection from nine different countries, fever (78%) and cough (57%) were also the most prevalent symptoms [18]. Although olfactory dysfunction (41%) was a relatively frequent symptom [19] in our study, it was relatively rare (2%).

Laboratory results showed that 56 (18.6%) patients had abnormal white blood cell counts, low platelet count (9.9%), elevated CRP (62.5%), and high d-dimer (26.2%). It has been suggested that raised CRP and d-dimer levels are linked to poor outcomes in patients with COVID-19 disease [20]. This information is critical for the diagnosis of COVID-19.

We found 13 asymptomatic patients (4.3%) with positive CT findings in nine cases (69%) and normal findings in four cases (31%). According to Inui S. et al. [21], "the incidence of normal chest CT findings in asymptomatic patients with COVID-19 is considerably high (an estimated 46% of patients)". "Low viral loads, confinement to the upper respiratory tract, and host factors are plausible explanations for negative chest CT findings in COVID-19 patients" [22,23].

Among the symptomatic group, 70 patients (23.3%) had normal CT findings. Ling Z. et al. found that 17% of their patients presented negative chest CT images at the initial presentation, and that a third of them who had a repeat CT scan became positive (after 3–6 days) for COVID-19 pneumonia. Two third of the patients showed persistent negative CT images (after 3–14 days). In our study, 68/70 patients with normal CT scan findings were found within 0 to 8 days of symptoms (Stages 1 and 2). This is relatively close to Ling Z. et al.'s [24] observation. The slightly higher percentage of negative scans in our study might reflect the massive screening effect in our population for the quick detection and isolation of positive cases. Chest CT was initially used as a quick screening method adjunct to PCR due to delayed PCR test results. "The WHO advised the use of chest imaging as part of the diagnostic workup of COVID-19 disease whenever RT-PCR testing was not

available, in case of delayed test results or when there was a clinical suspicion of COVID-19 with an initial negative RT-PCR testing" [25].

Mixed GGO with consolidations (70.6%) and pure GGO (44.2%) were the most common findings, followed by crazy paving (24.2%). These observations are slightly different from Salehi et al.'s, who found 31% and 88%, respectively [26]. We believe that the host's age and immune response play a significant role in these variables' imaging appearance. On the other hand, peripheral GGO distribution (100% vs. 76%) and bilateral involvement (91.3% vs. 87.5%) were very similar to Salehi et al.'s report [27]. We found only one 15-year-old symptomatic patient in Group A. They were the youngest patient with negative CT findings. This probably represents the low incidence of Covid-19 infection in this age group in our population. Group B (18-44 years) presented the highest number of negative CT findings (47/162-29%), followed by Group C (18/115) and Group D (4/23). These can be explained by a better immune response from relatively young individuals than from the elderly.

"Patients of the middle-aged group (45–59 years) and patients aged ≥ 60 years had more bilateral lung, lung lobe, and lung field involvements and greater lesion numbers than patients aged 18-44 years. The lesions were relatively more numerous in the lower lobe of both lungs and slightly higher in the right one. This finding may be related to the thick and short physiological structure of the right lower lobe bronchus, which may have allowed the virus to enter this area more easily. The peripheral involvement (100%) is probably due to the virus mainly affecting the terminal bronchioles and lung parenchyma around the respiratory bronchioles in the early stage" [27]. Bilateral lung involvement is common in all ages, while unilateral involvement is predominately a feature in younger/middle-aged patients.

In the early stage of symptomatic COVID-19 patients (0–4 days) and the progressive stage (5-8 days), 36.3% and 6.6% of the CT scans showed no abnormalities (which is consistent with Ref. 8). In case of CT abnormalities, peripheral mixed GGO with consolidation (63.3% and 83.5%, respectively) and pure GGO (55% and 36.5%, respectively) were the most important imaging manifestations, indicating that the disease may mainly invade the terminal respiratory bronchi or alveoli at first, before the

rapid progression of the disease with a poor prognosis or shorter course with a good prognosis [28].

In the peak (9-13 days) and late stages (14+ days), the CT features of the lesions were variable. The crazy-paving pattern, consolidation, and linear opacities increased significantly, indicating interstitial edema and alveolar exudation, which decreased thereafter. It has been reported that unilateral involvement is only present in the early and late phases [29]. It should also be noted that the temporal evolution and extent of lung abnormalities are heterogeneous among different patients, dependent on the severity of the disease [30,31,32].

The number of lesions per capita, the mean number of lesions in different lobes of both lungs, and the CT score were higher in Groups C (44-59 years) and D (>60 years) than in Group B (18-45 years). However, there was no significant difference in the number of lesions and in the mean CT score in the different age groups or between lungs/lung lobes ($P > 0.05$). We also observed a relatively greater number of lesions in both lower lobes than in the upper one and a smaller number of lesions in the right middle lobe in all age groups, which were also not statistically significant.

The same observation as in the distribution and number of lesions was reflected in the CT score in the different age groups and showed no significant difference in the mean scores between both lungs and different lobes in different groups.

5. CONCLUSION

COVID-19 has a diverse clinical presentation, course, and consequences. This also applies to the degree of pulmonary involvement. Comprehensive safety precautions must be taken before performing CT on patients who have COVID-19 whether it is suspected or confirmed. When evaluating for PE, low-radiation-dose chest imaging is advised unless CT pulmonary angiography is necessary. While some chest CT characteristics are frequently observed in COVID-19, others are not, which may aid in making a diagnosis. These characteristics include ground-glass opacities, vascular enlargement, bilateral abnormalities, lower lobe involvement, and posterior predominance.

The most common HRCT findings in patients with COVID-19 pneumonia were peripheral, bilateral, rounded pure ground glass opacities, and mixed GGO with consolidation. The early stages of the disease may reveal normal CT chest findings. Chest HRCT manifestations in patients with COVID-19 are related to the patient's age and the duration of their symptoms, and HRCT signs are relatively milder in younger patients and in the early stage of the disease. CT could serve as a useful tool for evaluating the changes of pulmonary abnormalities in patients at different stages and in different age groups (especially in elderly groups) for optimal management.

The appearance of COVID-19 on chest CT images follows a somewhat predictable pattern over time. Notably, asymptomatic patients with a SARS-CoV-2 infection frequently have normal chest CT examination results, and the proportion of symptomatic patients with COVID-19 and a normal chest CT examination is not negligible. Furthermore, lung abnormalities on chest CT images are nonspecific to COVID-19. Because of these limitations, chest CT should not be used as a stand-alone diagnostic tool to rule out or confirm COVID-19. The results of an RT-PCR test are the gold standard for such a diagnosis and a critical component in clinical decision-making.

Nonetheless, chest CT has been proposed to have potential value as a rapid triaging tool in patients with moderate to severe respiratory symptoms in a resource-constrained environment where COVID-19 is common. In addition, if an alternative diagnosis is suspected, a chest CT may be performed. Typical or indeterminate COVID-19 pneumonia features may be detected incidentally during a CT performed for another reason. In these cases, the interpreting radiologist should promptly discuss the possibility of COVID-19 with the referring physician. This information transfer can be facilitated by standardised reporting in accordance with guidelines such as those proposed by the RSNA. Additionally, a chest CT scan can be helpful in assessing patients who have deteriorated clinically for COVID-19 progression or secondary cardiac problems including ARDS, PE, superimposed pneumonia, or heart failure. Future research is required to establish the prognostic function of chest CT in COVID-19.

CONSENT

It is not applicable.

ETHICAL APPROVAL

As per international standard or university standard written ethical approval has been collected and preserved by the author(s).

COMPETING INTERESTS

Authors have declared that no competing interests exist.

REFERENCES

1. Report of clustering pneumonia of unknown etiology in wuhan city. Wuhan, China: Wuhan Municipal Health Commission; 2019. Google Scholar.
2. Mahase E. China coronavirus: WHO declares international emergency as death toll exceeds 200. *BMJ*. 2020; 368:m408. DOI: 10.1136/bmj.m408, PMID 32005727
3. AFP. UK PM pledges "infrastructure revolution" for coronavirus crisis [online]; n.d. *Khaleej Times*. Available: <https://www.khaleejtimes.com/coronavirus-pandemic/uk-pm-pledges-infrastructure-revolution-for-coronavirus-crisis>. Google Scholar
4. WHO. Coronavirus (COVID-19) dashboard. Available: https://covid19.who.int/?gclid=EAlalQobChMI2YXsxMmg8AIVguR3Ch3STgaaEAAYASABEgIHtfD_BwE
5. Chen Y, Li L. SARS-CoV-2: Virus dynamics and host response. *Lancet Infect Dis*. 2020;20(5):515-6. DOI: 10.1016/S1473-3099(20)30235-8, PMID 32213336.
6. Huang C, Wang Y, Li X et al. Clinical features of patients infected with 2019 novel coronavirus in Wuhan, China. *Lancet*. 2020;395(10223):497-506 Available: <https://doi.org/10.1016/s0140-6736.2020.01571-3>. PMID 31986264.
7. Kong WH, Li Y, Peng MW, Kong DG, Yang XB, Wang L, et al. SARS-CoV-2 detection in patients with influenza-like illness. *Nat Microbiol*. 2020;5(5):675-8. DOI: 10.1038/s41564-020-0713-1, PMID 32265517.
8. Yang Y, Yang M, Shen C et al. Evaluating the accuracy of different respiratory specimens in the laboratory diagnosis and monitoring the viral shedding of 2019-nCoV infections. 2020 Available: <https://doi.org/10.1101/2020.02.11.20021493>
9. Parry AH, Wani AH. Pulmonary embolism in coronavirus disease-19 (COVID-19) and use of compression ultrasonography in its optimal management. *Thromb Res*. 2020; 192:36. DOI: 10.1016/j.thromres.2020.05.022, PMID 32425262.
10. Chung M, Bernheim A, Mei X, Zhang N, Huang M, Zeng X et al. CT imaging features of 2019 novel coronavirus (2019-nCoV). *Radiology*. 2020; 202, 30;295(1):202-7. DOI: 10.1148/radiol.2020200230, PMID 32017661.
11. Radiology Scientific Expert Panel; Jeffrey P, Kanne Brent P, Little, Jonathan H, Chung Brett M, Elicker Loren H. *Ketaj essentials for radiologists on COVID-19*. An update; 2020.
12. Hansell DM, Bankier AA, MacMahon H, McLoud TC, Müller NL, Remy J. Fleischner Society Remy J. Glossary of terms for thoracic imaging. *Radiology*. 2008;246(3):697-722. DOI: 10.1148/radiol.2462070712, PMID 18195376.
13. Pan F, Ye T, Sun P, Gui S, Liang B, Li L et al. Time course of lung changes on chest CT during recovery from 2019 novel coronavirus (COVID-19) pneumonia. *Radiology*. 2020;295(3): 715-21. DOI: 10.1148/radiol.2020200370, PMID 32053470, Google Scholar.

14. Chang YC, Yu CJ, Chang SC, Galvin JR, Liu HM, Hsiao CH, et al. Pulmonary sequelae in convalescent patients after severe acute respiratory syndrome: Evaluation with thin-section CT. *Radiology*. 2005;236(3):1067-75. DOI: 10.1148/radiol.2363040958, PMID 16055695.
15. Ali ME, Alakkad A. Case study – an interesting case of COVID-19 induced fulminant myocarditis. *Asian J Res Cardiovasc Dis*. 2021;3(4):10-7.
16. Sungnak W, Huang N, Bécavin C, Berg M, Queen R, Litvinukova M, et al. SARS-CoV-2 entry factors are highly expressed in nasal epithelial cells together with innate immune genes. *Nat Med*. 2020;26(5):681-7. DOI: 10.1038/s41591-020-0868-6, Medline. PMID 32327758, Google Scholar.
17. Wang D, Hu B, Hu C, Zhu F, Liu X, Zhang J, et al. Clinical characteristics of 138 hospitalized patients with 2019 novel coronavirus–infected pneumonia in Wuhan, China. 2020;323(11):1061-9. DOI: 10.1001/jama.2020.1585 [online]. PMID 32031570.
18. Grant MC, Geoghegan L, Arbyn M, Mohammed Z, McGuinness L, Clarke EL, et al. The prevalence of symptoms in 24,410 adults infected by the novel coronavirus (SARS-CoV-2; COVID-19): A systematic review and meta-analysis of 148 studies from 9 countries. *PLOS ONE*. 2020;15(6):e0234765. DOI: 10.1371/journal.pone.0234765, PMID 32574165.
19. Agyeman AA, Chin KL, Landersdorfer CB, Liew D, Ofori-Asenso R. Smell and taste dysfunction in patients with COVID-19: A systematic review and meta-analysis. *Mayo Clin Proc*. 2020; 95(8):1621-31. DOI: ,Medline. PMID 32753137, Google Scholar.
20. Huang I, Pranata R, Lim MA, Oehadian A, Alisjahbana B. C-reactive protein, procalcitonin, D-dimer, and ferritin in severe coronavirus disease-2019: A meta-analysis. *Ther Adv Respir Dis*. 2020;14, p.175346662093717:1753466620937175. DOI: 10.1177/1753466620937175, PMID 32615866.
21. Inui S, Fujikawa A, Jitsu M, Kunishima N, Watanabe S, Suzuki Y, et al. Erratum: chest CT findings in cases from the cruise ship "Diamond Princess" with coronavirus disease 2019 (COVID-19). *Radiol Cardiothorac Imaging*. 2020;2(2):e204002. DOI: 10.1148/ryct.2020204002, PMID 33779623.
22. Sethuraman N, Jeremiah SS, Ryo A. Interpreting diagnostic tests for SARS-CoV-2. *JAMA*. 2020;323(22):2249-51. DOI: 10.1001/jama.2020.8259. Published online May 6. PMID 32374370, Google Scholar.
23. Wölfel R, Corman VM, Guggemos W, Seilmaier M, Zange S, Müller MA, et al. Virological assessment of hospitalized patients with COVID-2019. *Nature*. 2020;581(7809):465-9. DOI: 10.1038/s41586-020-2196-x, Medline. PMID 32235945, Google Scholar.
24. Ling Z, Xu X, Gan Q, Zhang L, Luo L, Tang X et al. Asymptomatic SARS-CoV-2 infected patients with persistent negative CT findings. *Eur J Radiol*. 2020;126:108956. DOI: 10.1016/j.ejrad.2020.108956.
25. Use of chest imaging in COVID19. Available:<https://www.who.int/publications/i/item/use-of-chest-imaging-in-covid-19>
26. Salehi S, Abedi A, Balakrishnan S, Gholamrezanezhad A. Coronavirus disease 2019 (COVID-19): A systematic review of imaging findings in 919 patients. *AJR Am J Roentgenol*, Volume 215. 2020;12020(215):1-7: 87-93. DOI: 10.2214/AJR.20.23034
27. Mehrjardi M, Kahkouee S, Pourabdollah M. Radio-pathological correlation of organizing pneumonia

- (OP): a pictorial review. Br J Radiol. 2017;90:(2016-07-23).
28. Ding X, Xu J, Zhou J, Long Q. Chest CT findings of COVID-19 pneumonia by duration of symptoms. Eur J Radiol. 2020 June;127:109009. DOI: 10.1016/j.ejrad.2020.109009, PMID 32325282.
29. Wang Y, Dong C, Hu Y, Li C, Ren Q, Zhang X, et al. Temporal changes of CT findings in 90 patients with COVID-19 pneumonia: A longitudinal study. Radiology. 2020;296(2):E55-64. DOI: 10.1148/radiol.2020200843, PMID 32191587.
30. Pan F, Ye T, Sun P, Gui S, Liang B, Li L, et al. Time course of lung changes at chest CT during recovery from coronavirus disease 2019 (COVID-19). Radiology. 2020;295(3):715-21. DOI: 10.1148/radiol.2020200370, PMID 32053470.
31. Pan Y, Guan H, Zhou S, et al. Initial CT findings and temporal changes in patients with the novel coronavirus pneumonia (2019-nCoV): a study of 63 patients in Wuhan, China. Eur Radiol. 2020;30(6):3306-9. DOI: Medline. PMID 32055945, Google Scholar.
32. Yu M, Xu D, Lan L, Tu M, Liao R, Cai S, et al. Thin-section chest CT Imaging of coronavirus disease 2019 pneumonia: comparison between patients with mild and severe disease. Radiol Cardiothorac Imaging. 2020; 2(2):e200126. DOI: 10.1148/ryct.2020200126, PMID 33778568.

© 2022 Chakraborty et al.; This is an Open Access article distributed under the terms of the Creative Commons Attribution License (<http://creativecommons.org/licenses/by/4.0>), which permits unrestricted use, distribution, and reproduction in any medium, provided the original work is properly cited.

Peer-review history:
The peer review history for this paper can be accessed here:
<https://www.sdiarticle5.com/review-history/92709>